JOURNAL OF SPACECRAFT AND ROCKETS
Vol. 45, No. 1, January–February 2008

Electric Sail Performance Analysis

Giovanni Mengali* and Alessandro A. Quarta†
University of Pisa, 56122 Pisa, Italy
and
Pekka Janhunen‡
Finnish Meteorological Institute, 00101 Helsinki, Finland

DOI: 10.2514/1.31769

An electric sail uses the solar wind dynamic pressure to produce a small but continuous thrust by interacting with an electric field generated around a number of charged tethers. Because of the weakness of the solar wind dynamic pressure, quantifiable in about 2 nPa at Earth's distance from the sun, the required tether length is of the order of some kilometers. Equipping a 100-kg spacecraft with 100 of such tethers, each one being of 10-km length, is sufficient to obtain a spacecraft acceleration of about 1 $\mathrm{mm/s^2}$. These values render the electric sail a potentially competitive propulsion means for future mission applications. The aim of this paper is to provide a preliminary analysis of the electric sail performance and to investigate the capabilities of this propulsion system in performing interplanetary missions. To this end, the minimum-time rendezvous/transfer problem between circular and coplanar orbits is considered, and an optimal steering law is found using an indirect approach. The main differences between electric sail and solar sail performances are also emphasized.

Nomenclature

a	=	propulsive acceleration
e	=	elementary charge, 1.602176×10^{-19} C
H	=	Hamiltonian
$\hat{\boldsymbol{\imath}}$	=	unit vector
k_t	=	coefficient of a multiline tether
L	=	total tether length
m	=	spacecraft total mass
m_b	=	spacecraft body mass
m_e	=	electron mass, 9.109382×10^{-31} kg
m_p	=	proton mass, 1.672621×10^{-27} kg
m_{pay}	=	payload mass
m_t	=	tether mass
n	=	solar wind electron density
$\boldsymbol{r}$	=	sun–spacecraft position vector, $r \triangleq \|\boldsymbol{r}\|$
r_w	=	cylindrical wire radius
T_e	=	solar wind electron temperature in energy units
t	=	time
V	=	wire potential
v	=	velocity
α	=	thrust angle
α_λ	=	primer vector thrust angle
β	=	spacecraft mass-to-power ratio
ϵ_0	=	permittivity of vacuum, 8.854187×10^{-12} F/m
η	=	payload mass fraction
λ	=	adjoint variable
μ	=	gravitational parameter
θ	=	polar angle
ρ_w	=	wire mass density
σ_x	=	value of x per unit length of tether
τ	=	switching parameter

Subscripts

e	=	electron
f	=	final
max	=	maximum
n	=	normal to the nominal spin plane
p	=	proton
r	=	radial
sw	=	solar wind
θ	=	circumferential
0	=	initial
$\oplus$	=	Earth
$\odot$	=	sun
$\mathrm{♀}$	=	Mars
$\mathrm{♂}$	=	Venus

Superscripts

$\cdot$	=	time derivative
$\tilde{}$	=	approximated value
$\star$	=	optimal value

Introduction

AN ELECTRIC sail is an innovative propulsion concept that, similar to a more conventional solar sail, allows a spacecraft to perform high-energy orbit transfer maneuvers without the need for reaction mass. Because electric sails can operate nominally over indefinitely long periods, the achievable energy changes are substantial, greater than those possible with conventional (either chemical or electrical) propulsion systems.

The fundamental electric sail concept was devised by Janhunen in 2004 [1] and then refined in a recent paper [2]. The basic idea consists in spinning the spacecraft around an axis and using the rotational motion to deploy a number (on the order of 100) of long conducting tethers. These are connected to a solar-powered electron gun for which the aim is to maintain the tethers at a high (up to 20 kV) positive potential. The electric field generated by the tethers behaves like a shield for the solar wind ions that, impacting on it, generate a low but continuous thrust. To prevent the lifetime reduction of a single-line tether caused by the impact with meteoroids or orbital debris, each tether is composed of multiple wires with redundant interlinking (referred to as Hoytether [3]), according to the project developed by Forward and Hoyt [4]. The Hoytether technology has been developed in the framework of tether transport systems and has

Received 24 April 2007; accepted for publication 4 October 2007.

*Associate Professor, Department of Aerospace Engineering; g.mengali@ing.unipi.it. Member AIAA.
†Research Assistant, Department of Aerospace Engineering; a.quarta@ing.unipi.it. Member AIAA.
‡Senior Researcher, Space Research; pekka.janhunen@fmi.fi.

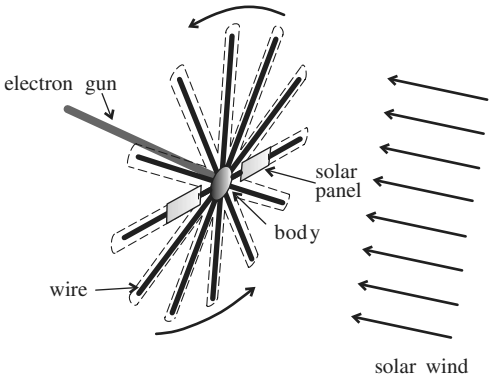

Fig. 1 Conceptual sketch of an electric sail.

been proposed as a key element in a number of space missions [5–7]. The tether width for a typical electric sail application is about 2 cm and is composed of wires for which the diameter is 20 μm. Successful tests conducted recently (July 2007) at the University of Helsinki have verified the feasibility of bonding a 25-μm-diam wire. Therefore, a diameter value of 20 μm for the electric sail wires appears compatible with the current or near-term technology.

Assuming a 100-kg spacecraft with 100 such tethers, each being of 10-km length, the electric sail provides about 0.1-N thrust at 1-AU distance from the sun. Unlike solar sails, for which the propelling thrust varies as the inverse square distance from the sun, the electric sail thrust force decays as $(1/r)^{7/6}$ (see [2]).

Once deployed, the tethers are maintained stretched by rotating the spacecraft with a spin period of about 20 min and lie on the same plane (the spin plane). The electricity needed to power the electron gun is obtained from conventional, modest-sized, solar panels. A conceptual sketch of an electric sail is shown in Fig. 1.

The thrust produced by the solar wind on the tethers has been predicted by simulation and theory [2]. It is typically on the order of 50–100 nN/m and depends on the solar wind conditions (in terms of both density and speed) and on the tether potential (the thrust increases with the potential). The dynamic pressure of the solar wind is, on average, about 2 nPa at 1-AU distance from the sun and is about 5000 times smaller than the radiation pressure of the solar photons that provide the momentum source used by a solar sail. Therefore, one might think that the obtainable performance (in terms of acceleration) of an electric sail is much less than that of a solar sail. However, when compared with a two-dimensional membrane surface, a charged and thin tether can be built extremely lightweight per effective sail area produced. This is possible because the effective "electric width" of a charged tether is about 20 m (a few times the plasma Debye length in the solar wind), a dimension for which the order is one million times larger than the physical thickness of the wire.

A space mission based on an electric sail propulsion system requires that the sail plane attitude may be varied to turn the thrust direction. To this end, a potentiometer (that is, a tunable resistor) is placed between the spacecraft and each tether. Because the thrust magnitude depends on the tether potential, the latter can be slightly changed through the potentiometer. As a result, the tether spin plane can be turned by modulating the potentiometer setting with a sinusoidal signal synchronized to the sail rotation. In particular, the phase of the signal defines the turn direction and its amplitude determines how fast the plane rotation occurs.

When the sail plane is oriented normal to the solar wind, a radial thrust is obtained with respect to the sun–spacecraft direction. However, a circumferential component can also be generated by inclining the sail plane at an angle with respect to the nearly radial solar wind flow. The corresponding thrust angle α (that is, the angle between the net thrust and the radial direction) is approximately equal to one-half the sail plane's inclination angle. Although the maximum value of α is not known with confidence, we estimate that it may reach a value ranging between 20 and 35 deg. The presence of an upper constraint on $\alpha_{\max}$ is justified by the necessity of preventing possible mechanical instabilities, even if the occurrence of a critical behavior for $\alpha > \alpha_{\max}$ still deserves a more detailed investigation.

Unlike solar sails, one of the operational benefits of an electric sail is that the thrust magnitude and direction can be independently controlled within some limits. Another interesting feature is the possibility of introducing coasting arcs in the spacecraft trajectory without the need for attitude maneuvers. In fact, the electric sail thrust can be turned on or off at any time by simply switching on or off the electron gun. The finite capacitance of the tethers causes only a corresponding delay on thrust modulation of a few tens of seconds.

The aim of this paper is to characterize the electric sail performance and to analyze the capabilities of this propulsion system in performing interplanetary missions. For mathematical tractability, and in accordance with a preliminary mission analysis, we introduce the substantial simplification of a constant value for the solar wind velocity. The electric sail thrust level, of course, depends on the solar wind properties, which actually are variable and cannot be reliably predicted beforehand. Nevertheless, these uncertainties can be compensated for by the electric thrust control: that is, by adjusting the electron-gun current and voltage to counteract the thrust changes due to the solar wind variations.

The paper is organized as follows. The mathematical model characterizing the propulsive thrust as a function of the main design variables is first described. Then a mass breakdown model is introduced to account for the contribution of payload, spacecraft body, and tethers to the total spacecraft mass. This allows one to quantify to first order the dependence of the spacecraft propulsive acceleration on the main design parameters (wire radius, length, and wire potential) and on the payload mass fraction. The electric sail performance is then investigated by considering a classical minimum-time, circle-to-circle, two-dimensional transfer. Finally, a performance comparison with a flat solar sail is discussed.

Thruster Mathematical Model

Consider a tether of length L charged at a potential V and plunged in the solar wind. The electric field generated around the tether interacts with the solar wind in such a way that a small thrust is obtained. It may be shown [2] that the propulsive force per unit of tether length is

$$\sigma_F = \frac{6.18 m_p v_{\rm sw}^2 \sqrt{n\epsilon_0 T_e}}{e\sqrt{\exp\left[\dfrac{m_p v_{\rm sw}^2}{eV}\ell_n\left(\dfrac{2}{r_w}\sqrt{\dfrac{\epsilon_0 T_e}{ne^2}}\right)\right]-1}} \tag{1}$$

Although the solar wind velocity $v_{\rm sw}$ is actually a function of the distance r from the sun [8], in this paper, we use the simplified approximation of considering a constant value for the solar wind velocity [2]: that is, $v_{\rm sw} \cong 400$ km/s. In Eq. (1), n and T_e depend on r as

$$n = n_\oplus \left(\frac{r_\oplus}{r}\right)^2 \tag{2}$$

and

$$T_e = T_{e_\oplus}\left(\frac{r_\oplus}{r}\right)^{1/3} \tag{3}$$

where $n_\oplus = 7.3 \times 10^6$ m^{-3} is the mean solar wind electron density at $r_\oplus \triangleq 1$ AU, and $T_{e_\oplus} = 12$ eV is the corresponding mean solar wind electron temperature [9,10]. As a result, σ_F is a function of the distance r from the sun [via Eqs. (2) and (3)] and of the two design parameters V and r_w.

If one neglects the dependence on r in the logarithm argument of Eq. (1), the following approximate expression for the propulsive force is found [2]:

$$\sigma_F \cong \widetilde{\sigma}_F \triangleq \sigma_{F_\oplus}\left(\frac{r_\oplus}{r}\right)^{7/6} \tag{4}$$

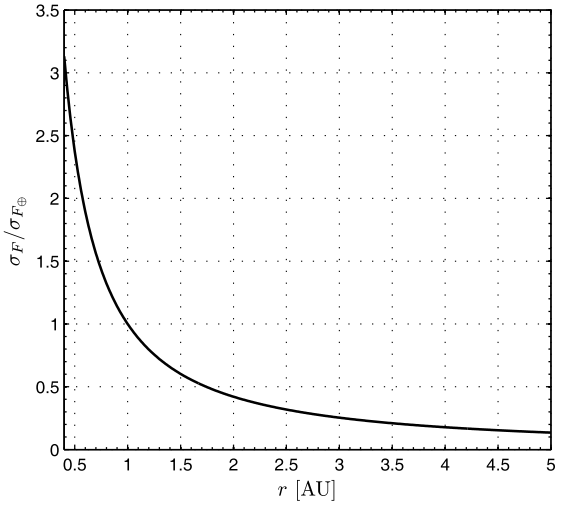

a) Dimensionless propulsive force

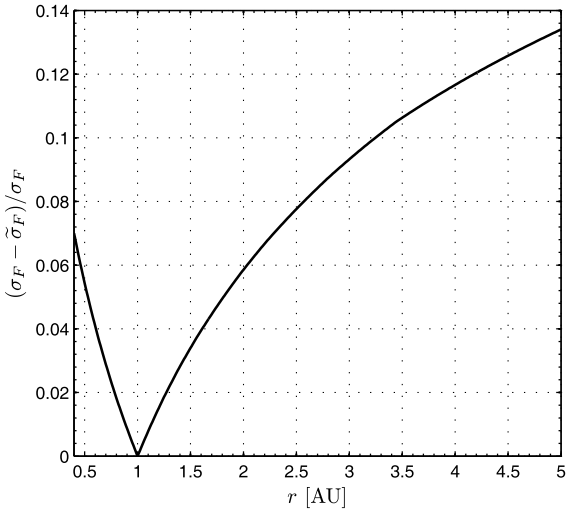

b) Accuracy of the simplified model, [see Eq. (4)]

Fig. 2 Propulsive force as a function of the sun's distance.

which states that the propulsive force reduces with the sun–spacecraft distance as $r^{-7/6}$. Note that $\sigma_{F_\oplus}$ is the value of σ_F calculated from Eq. (1) when $r = 1$ AU. Assuming a wire radius $r_w = 10$ μm, and a potential $V = 12$ kV [2], Fig. 2 shows that the approximate thrust model of Eq. (4) matches the accurate model of Eq. (1) to within 4% for both Earth–Venus and Earth–Mars transfers.

Spacecraft Acceleration

A mass distribution model is now introduced to obtain an estimate of the spacecraft acceleration. Specifically, the following mass breakdown is assumed:

$$m = m_b + m_t + m_{\text{pay}} \tag{5}$$

where m_b is the mass of the spacecraft body (including structures, electron gun, and electronics), and m_t comprises the total length of tethers used for the electric sail.

The value of m_b per unit length of tether, referred to as σ_{m_b}, is a function of the applied voltage V of the characteristic dimension r_w of each wire constituting the tether and of the mass-to-power ratio β, according to the following relationship [2]:

$$\sigma_{m_b} = 2k_t\beta n_\oplus r_w\sqrt{\frac{2e^3V^3}{m_e}} \tag{6}$$

where k_t is a coefficient that models the interaction between the different wires of a multiline tether [4]. For example, $k_t = 4.3$ for a tether constituted by four wires.

The mass-to-power ratio can be estimated using statistical data, on the base of the current technology. In particular, for all of the following simulations, we assume $\beta = 0.25$ kg/W, a reference (and conservative) value compatible with that used in the SMART-1 mission [11,12].

The tether mass per unit length is

$$\sigma_{m_t} = k_t\pi\rho_w r_w^2 \tag{7}$$

where a value $\rho_w = 4000$ kg/m^3 is assumed (this corresponds to aluminum alloyed with copper or some other heavier metal). Denoting the payload mass as a fraction of the total spacecraft mass, $\eta \triangleq m_{\text{pay}}/m$, from Eqs. (5–7), one has

$$\sigma_m = \frac{k_t}{1-\eta}\left(2\beta n_\oplus r_w\sqrt{\frac{2e^3V^3}{m_e}} + \pi\rho_w r_w^2\right) \tag{8}$$

The modulus of spacecraft propulsive acceleration, at a distance r from the sun, is given by the ratio between σ_F and σ_m: that is,

$$a = \frac{\sigma_F}{\sigma_m} \cong a_\oplus\left(\frac{r_\oplus}{r}\right)^{7/6} \tag{9}$$

where

$$a_\oplus \triangleq \frac{6.18(1-\eta)m_p v_{\text{sw}}^2\sqrt{n_\oplus\epsilon_0 T_{e_\oplus}}}{ek_t\left(2\beta n_\oplus r_w\sqrt{\frac{2e^3V^3}{m_e}} + \pi\rho_w r_w^2\right)\sqrt{\exp\left[\frac{m_p v_{\text{sw}}^2}{eV}\ell_n\left(\frac{2}{r_w}\sqrt{\frac{\epsilon_0 T_{e_\oplus}}{n_\oplus e^2}}\right)\right] - 1}} \tag{10}$$

Therefore, after the tether material ρ_w and its configuration k_t are chosen, the ratio $a_\oplus/(1-\eta)$ depends on the voltage V and on the radius r_w of each wire only. The isocontour lines for the sail propulsive acceleration at 1 AU are shown in Fig. 3 in dimensionless form ($a_\oplus$ was divided by the sun's gravitational acceleration $a_\odot \triangleq \mu_\odot/r_\oplus^2 \cong 5.93$ mm/s^2). From Fig. 3, it is clear that for a given value of r_w, there exists an optimal voltage value $V = V^\star$ that maximizes the propulsive acceleration. The dependence of $V^\star$ on the wire radius for $r_w \in [5, 30]$ μm is shown in Fig. 4. A quadratic polynomial in the form

$$V^\star = b_2 r_w^2 + b_1 r_w + b_0 \tag{11}$$

is found to best-fit approximate (with errors less than 1.5%) the relationship $V^\star = V^\star(r_w)$. The recommended coefficients b_0, b_1, and b_2 for curve-fitting are given in Table 1. When the optimal

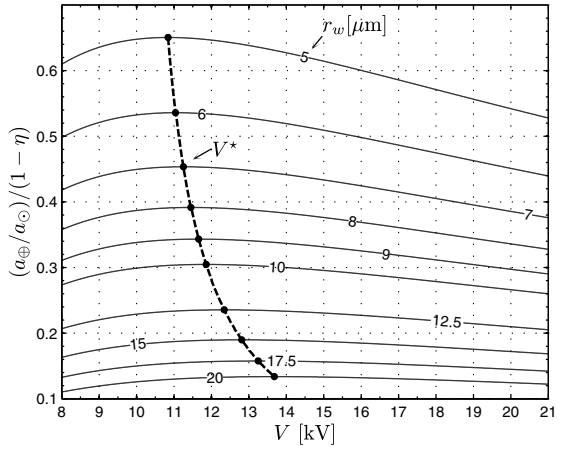

Fig. 3 Dimensionless propulsive acceleration at 1 AU [see Eq. (10)].

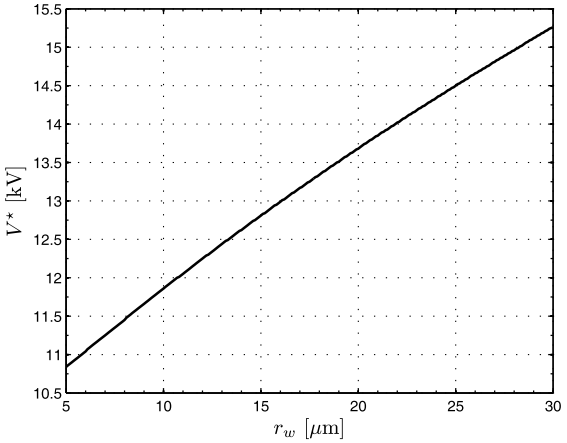

Fig. 4 Optimal tether voltage.

voltage value of Eq. (11) is substituted into Eq. (10), the latter becomes a function of the design variable r_w only. This function, which is drawn in Fig. 5, can be accurately approximated through a rational relationship in the following form:

$$a_\oplus = \frac{a_\odot(1-\eta)}{c_2 r_w^2 + c_1 r_w + c_0} \tag{12}$$

where the coefficients c_0, c_1, and c_2 are given in Table 1. Note,

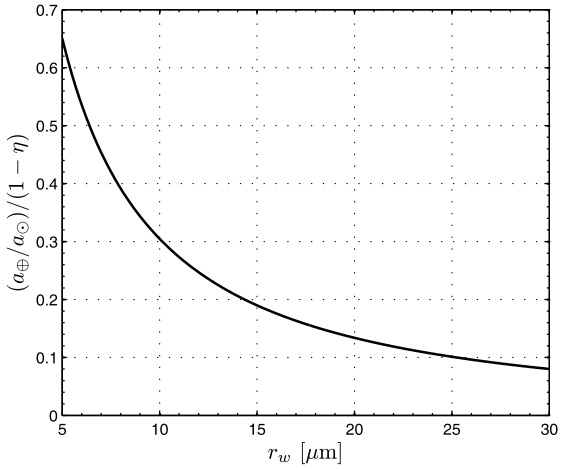

Fig. 5 Optimal dimensionless propulsive acceleration at 1 AU [see Eq. (12)].

Table 1 Best-fit interpolation coefficients [see Eqs. (11) and (12)].

Coefficient	Value
b_0	9.76 kV
b_1	0.2227 kV/μm
b_2	-1.319×10^{-3} kV/μm^2
c_0	1.6752×10^{-2}
c_1	0.28095 μm^{-1}
c_2	4.568×10^{-3} μm^{-2}

however, that the coefficients in Table 1 are not universal in the sense that they depend on the value of the mass-to-power ratio β.

To summarize, when the payload mass and the wire radius are fixed, and under the assumption that the optimal voltage value is taken ($V = V^\star$), the spacecraft mass per unit length is given by Eq. (8), and Eq. (12) provides the relationship between the payload mass fraction and the value of the propulsive acceleration at 1 AU.

The total tether length L can be calculated as

$$L = \frac{m_{\text{pay}}}{\eta \sigma_m} \tag{13}$$

Equation (13) is drawn in Fig. 6 for different values of the payload mass fraction. For example, assuming a payload mass $m_{\text{pay}} = 100$ kg and 100 tethers, the length of each tether is $1550/100 = 15.5$ km. This length is compatible with a tether transport system for applications dedicated to interplanetary transfers [5] or orbital raising [6,7].

It may be shown that the power required to maintain the tether potential can be supplied by conventional, modest-sized, solar panels. In fact, assuming an average solar wind density $n = 7.3$ cm^{-3}, a wire radius $r_w = 10$ mm, and an electron-gun potential of 20 kV, from Eq. (9) of [2] one obtains a current per unit length equal to 1.96 nA/m. Multiplying this value by $k_t = 4.3$ to account for the multiple-wire Hoytether structure and by the total length of 1550 km, one has a current of 13 mA. Multiplying this current by the electron-gun potential and assuming an efficiency of the electron gun of 90%, one obtains that the power required by solar panels is about 290 W.

An interesting comparison with a conventional solar sail can now be made. Assuming, for example, a wire radius $r_w = 10$ μm and a propulsive acceleration $a_\oplus = 0.5$ mm/s^2, Eq. (12) provides a payload mass fraction $\eta \cong 72.3\%$. This value is substantially greater than that achievable with a solar sail [13]. For comparative purposes, consider a square, high-performance, and perfectly reflecting solar sail having a characteristic acceleration 0.5 mm/s^2 and a sail assembly loading of 10 g/m^2 [13]. Using the mass breakdown model proposed in [14], it may be shown that the solar sail side length is about 100 mm and the payload mass fraction is 45.2%, with a percentage decrease of 37.5% with respect to an electric sail.

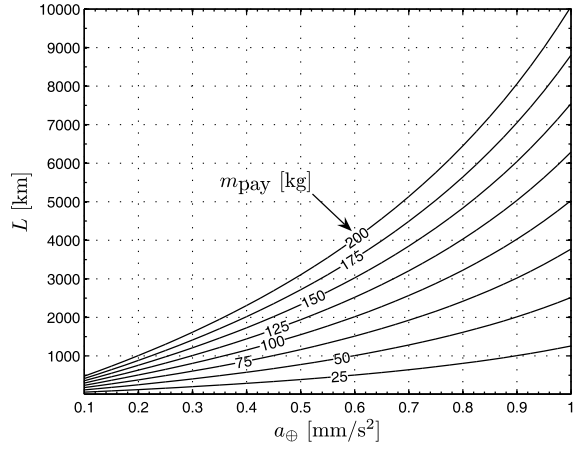

Fig. 6 Total tether length ($r_w = 10$ μm).

Electric Sail Performance

The performance of an electric sail can now be thoroughly investigated by studying the minimum-time transfer problem between circular and coplanar orbits. To this end, we start our analysis from the heliocentric equations of motion for an electric sail in a polar inertial frame $\mathcal{T}_\odot(r,\theta)$. Bearing in mind that the sail acceleration is given by Eq. (9), one has

$$\dot{r} = v_r \tag{14}$$

$$\dot{\theta} = \frac{v_\theta}{r} \tag{15}$$

$$\dot{v}_r = \frac{v_\theta^2}{r} - \frac{\mu_\odot}{r^2} + a_\oplus \tau \cos\alpha \left(\frac{r_\oplus}{r}\right)^{7/6} \tag{16}$$

$$\dot{v}_\theta = -\frac{v_r v_\theta}{r} + a_\oplus \tau \sin\alpha \left(\frac{r_\oplus}{r}\right)^{7/6} \tag{17}$$

where the sail polar angle θ is measured anticlockwise from some reference position (see Fig. 7), and $\alpha \in [-\alpha_{\max}, \alpha_{\max}]$. The switching parameter $\tau = (0,1)$ models the thruster on/off condition and is introduced to account for coasting arcs in the spacecraft trajectory. As stated, we look for the minimum time

$$t_f^\star \triangleq \min(t_f) \tag{18}$$

necessary to perform a circle-to-circle orbit transfer. At the initial time $t_0 = 0$, the electric sail state is given by

$$r(0) = r_\oplus, \qquad \theta(0) = v_r(0) = 0, \qquad v_\theta(0) = \sqrt{\mu_\odot / r_\oplus} \tag{19}$$

Conditions (19) are representative of an electric sail deployment on a parabolic Earth-escape trajectory: that is, with zero hyperbolic excess energy ($C_3 = 0$ km^2/s^2).

The minimum time $t_f^\star$ is calculated by means of an indirect approach. The Hamiltonian function is

$$H = \lambda_r v_r + \lambda_\theta \frac{v_\theta}{r} + \lambda_{v_r}\left(\frac{v_\theta^2}{r} - \frac{\mu_\odot}{r^2}\right) - \lambda_{v_\theta}\frac{v_r v_\theta}{r} + a_\oplus \tau (\lambda_{v_r}\cos\alpha + \lambda_{v_\theta}\sin\alpha)\left(\frac{r_\oplus}{r}\right)^{7/6} \tag{20}$$

where λ_i is the adjoint variable associated with the state variable i. The corresponding time derivatives $\dot{\lambda}_i = -\partial H/\partial i$ are provided by the following Euler–Lagrange equations:

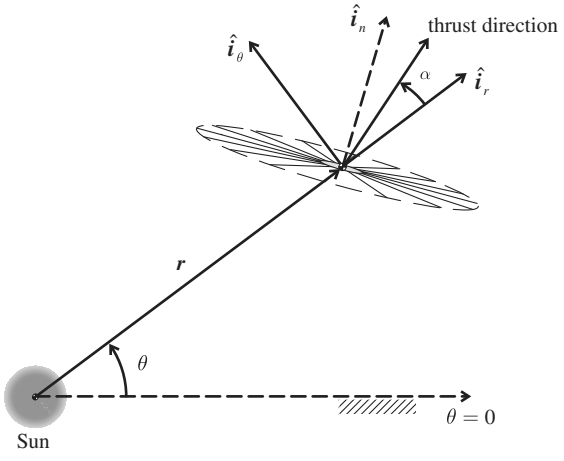

Fig. 7 Reference frame and thrust angle.

$$\dot{\lambda}_r = \frac{\lambda_\theta v_\theta}{r^2} + \lambda_{v_r}\left(\frac{v_\theta^2}{r^2} - \frac{2\mu_\odot}{r_i^3}\right) - \lambda_{v_\theta}\frac{v_r v_\theta}{r^2} + \frac{7 a_\oplus \tau}{6r}\left(\frac{r_\oplus}{r}\right)^{7/6}(\lambda_{v_r}\cos\alpha + \lambda_{v_\theta}\sin\alpha) \tag{21}$$

$$\dot{\lambda}_{\theta_i} = 0 \tag{22}$$

$$\dot{\lambda}_{v_r} = -\lambda_r + \lambda_{v_\theta}\frac{v_\theta}{r} \tag{23}$$

$$\dot{\lambda}_{v_\theta} = -\frac{\lambda_\theta}{r} - 2\frac{\lambda_{v_r} v_\theta}{r} + \frac{\lambda_{v_\theta} v_r}{r} \tag{24}$$

The final boundary conditions for a circle-to-circle rendezvous problem are

$$r_i(t_f) = r_f, \qquad v_r(t_f) = \lambda_\theta(t_f) = 0, \qquad v_\theta(t_f) = \sqrt{\mu_\odot / r_f} \tag{25}$$

where r_f is the target orbit radius. The final polar angle $\theta(t_f)$ is left free and is an output of the optimization process. Finally, the minimum flight time is obtained by enforcing [15] the transversality condition $H(t_f) = 1$.

From Pontryagin's maximum principle, an optimal steering law is found by maximizing, at all times, the Hamiltonian function. The result is

$$\alpha = \begin{cases} \text{sign}(\lambda_{v_\theta})\alpha_\lambda & \text{if } \alpha_\lambda \le \alpha_{\max} \\ \text{sign}(\lambda_{v_\theta})\alpha_{\max} & \text{if } \alpha_\lambda > \alpha_{\max} \end{cases} \tag{26}$$

where $\alpha_\lambda \in [0, \pi]$ is defined as

$$\alpha_\lambda \triangleq \arccos\left(\frac{\lambda_{v_r}}{\sqrt{\lambda_{v_r}^2 + \lambda_{v_\theta}^2}}\right) \tag{27}$$

Note that if one removes the constraint on $\alpha_{\max}$ (which amounts to saying that $\alpha_{\max} = \pi$), Eqs. (26) and (27) reduce to Lawden's primer vector control law [16,17]. Because H depends linearly on τ, a bang-bang control law for the switching parameter is optimal, or

$$\tau = \begin{cases} 0 & \text{if } (\lambda_{v_r}\cos\alpha + \lambda_{v_\theta}\sin\alpha) \le 0 \\ 1 & \text{if } (\lambda_{v_r}\cos\alpha + \lambda_{v_\theta}\sin\alpha) > 0 \end{cases} \tag{28}$$

where α is given by Eq. (26).

Numerical Simulations

A number of missions have been simulated by varying the spacecraft propulsive acceleration at 1 AU in the range $a_\oplus \in [0.5, 6]$ mm/s^2 and the maximum thrust angle in the range $\alpha_{\max} \in [20, 35]$ deg. In particular, missions toward Mars ($r_f = r_\mars \triangleq 1.52368$ AU) and Venus ($r_f = r_\venus \triangleq 0.723332$ AU) have been investigated.

The minimum-time rendezvous problem was solved using a set of canonical units in the integration of the differential equations to reduce their numerical sensitivity. The differential equations were integrated in double-precision using a Runge–Kutta fifth-order scheme with absolute and relative errors of 10^{-6}. The final boundary constraints were set to 100 km for the position error and 0.1 m/s for the velocity error. These tolerance limits are consistent for purposes of preliminary mission analysis. In fact, the electric sail cannot operate in the planet's magnetosphere because it uses the solar wind to generate the propulsive acceleration.

The simulation results have been summarized in Fig. 8. Recall from equations of motion (16) and (17) that the electric sail performance is fully specified after the value of $a_\oplus$ is given. In

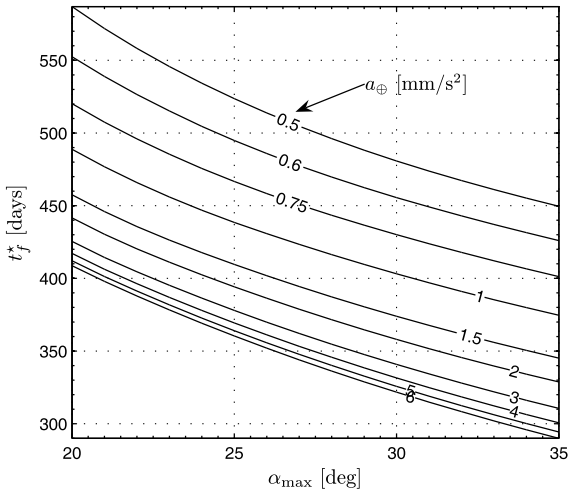

a) Earth–Mars transfer

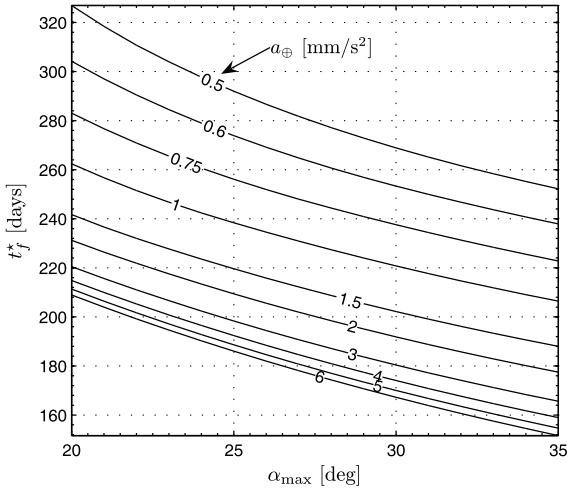

b) Earth–Venus transfer

Fig. 8 Minimum-time circle-to-circle rendezvous.

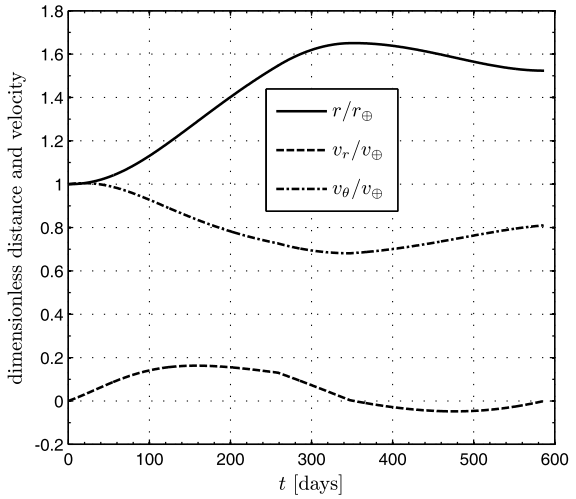

a) Time histories of distance and velocity

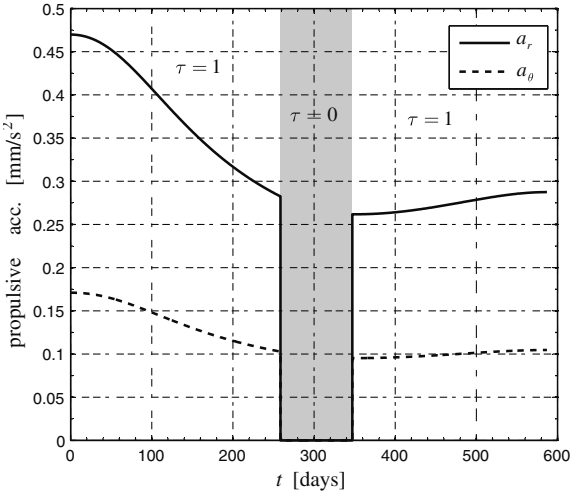

b) Acceleration components

Fig. 9 Earth–Mars circle-to-circle rendezvous with $a_\oplus = 0.5$ mm/s^2 and $\alpha_{\max} = 20$ deg.

particular, using values representative of a low-performance electric sail (for example, $a_\oplus = 0.5$ mm/s^2 and $\alpha_{\max} = 20$ deg), an Earth–Mars mission can be completed in 587 days and an Earth–Venus mission can be completed in 327 days.

The details for an Earth–Mars mission are shown in Fig. 9. Note that the optimal trajectory (illustrated in Fig. 10) includes a coasting arc ($\tau = 0$) for which the length is about 85 days. During the two propelled arcs, the optimal thrust angle coincides, at all times, with its maximum allowed value $\alpha_{\max} = 20$ deg. Also, Fig. 11 shows that the required sail angular rate (calculated with respect to an inertial frame) is always less than 1 deg/day for the sample mission.

Figure 8 shows that the sensitivity of $t_f^\star$ to the propulsive acceleration at 1 AU increases as long as $a_\oplus$ is decreased. Because, for a given tether length, m_{pay} is inversely proportional to $a_\oplus$ (see Fig. 6), it is also interesting to calculate the optimal transfer times for small values of $a_\oplus$. Assuming an Earth–Mars transfer and $\alpha_{\max} = (20, 30)$ deg, the simulation results are shown in Fig. 12. For comparative purposes, Fig. 12 also shows the minimum times corresponding to a flat solar sail with an optical force model [18–20]. In this latter case, $a_\oplus$ coincides with the solar sail characteristic acceleration: that is, the maximum sail acceleration at 1 AU. The minimum times have a substantial increase for $a_\oplus < 0.4$ mm/s^2 and, as expected, $t_f^\star(a_\oplus)$ has a vertical asymptote as $a_\oplus \to 0$.

Figure 12 shows that there exists a value ($a_\oplus \cong 0.55$ mm^2/s^2 for $\alpha_{\max} = 20$ deg and $a_\oplus \cong 1.6$ mm/s^2 for $\alpha_{\max} = 30$ deg) beyond which the solar sail performance is superior to the electrical sail. At a first glance this result might seem surprising because the electric sail,

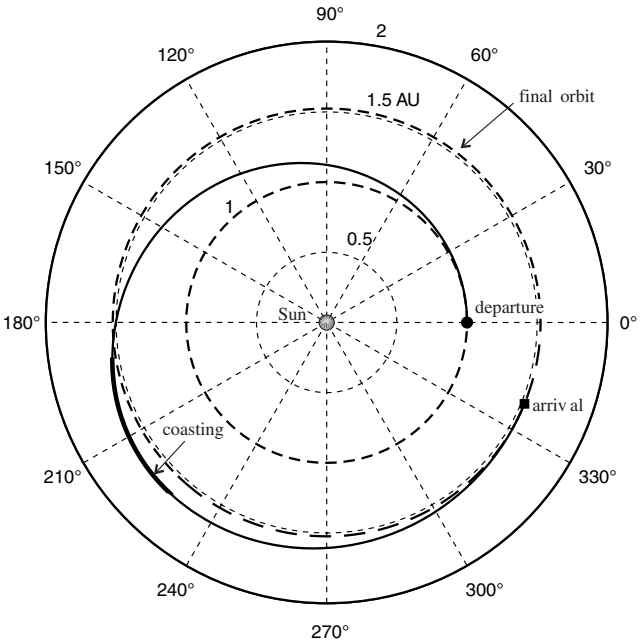

Fig. 10 Optimal trajectory for an Earth–Mars transfer using an electric sail.

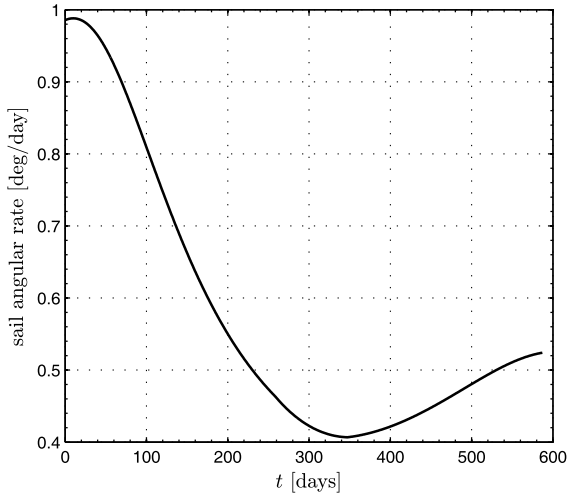

Fig. 11 Sail angular rate for an Earth–Mars circle-to-circle transfer.

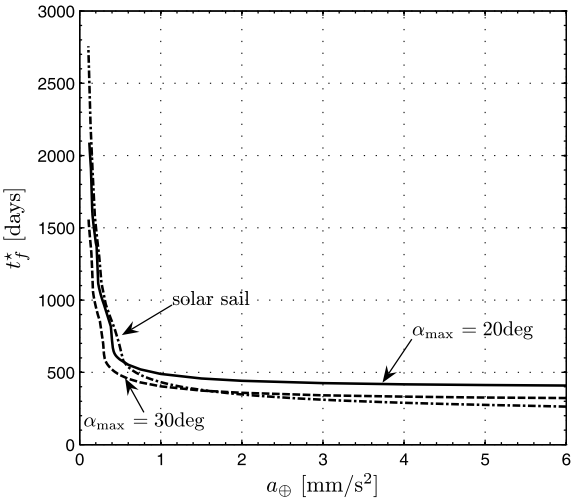

Fig. 12 Minimum-time Earth–Mars transfer as a function of $a_\oplus$.

$a_\oplus$ being equal, has a higher propulsive acceleration than a solar sail for $r > r_\oplus$. In fact, although the solar sail thrust decreases as the inverse square distance from the sun, the electric sail thrust has a smaller reduction, described by Eq. (9). Nevertheless, the better solar sail performance can be explained by the fact that the solar sail SS has a much higher capability of orienting the thrust [18] and generating a circumferential thrust component than the electric sail ES, or $\alpha_{\max}(\mathrm{SS}) \gg \alpha_{\max}(\mathrm{ES})$.

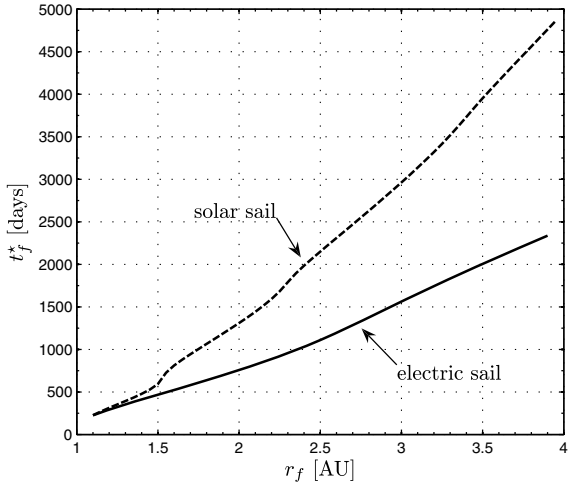

Fig. 13 Minimum transfer times for an electric sail ($a_\oplus = 0.5$ mm/s^2 and $\alpha_{\max} = 30$ deg) and a solar sail.

Finally, the performance of an electric sail was investigated as a function of the final orbit radius in the range $r_f \in [1.1, 4]$ AU with $a_\oplus = 0.5$ mm/s^2 and $\alpha_{\max} = 30$ deg. The simulation results have been summarized in Fig. 13 and compared with the performance obtainable with a flat solar sail with an optical force model and a characteristic acceleration equal to 0.5 mm/s^2. Although more refined mathematical models and experimental evidence are necessary in support of these simulations, the obtainable reduction in mission times suggests that the electric sail may represent a promising option for future space missions.

Conclusions

The electric field generated around an electric sail, interacting with the solar wind, produces a low thrust that can be used as a spacecraft propulsion system. The resulting thrust can be oriented, within some limits, by inclining the normal to the electric sail spin plain with respect to the sun–spacecraft direction, thus creating a circumferential thrust component. Because the maximum inclination angle of the electric sail is constrained to not exceed a prescribed maximum angle, it is important to investigate the limitations that this constraint poses on the spacecraft maneuver capabilities. To quantify this effect, we analyzed the problem of minimum-time rendezvous between circular and coplanar orbits. The problem was solved using an indirect approach and the resulting optimal control law was applied to study rendezvous missions to Mars and Venus. A reasonable comparison between an electric sail and a more conventional solar sail system was established in terms of payload mass fraction deliverable for a given mission. Assuming the same value of characteristic acceleration for the two sails, an electric sail is potentially superior to a solar sail both in terms of payload mass fraction deliverable and in terms of thrust magnitude at a given solar distance. Although the electric sail still deserves more refined theoretical and experimental studies, the proposed study represents a first step toward substantiating this propulsion concept in terms of preliminary mission design.

Acknowledgments

The research of the first two authors was financed in part by the Italian Ministry of Education, University and Research. The third author acknowledges the Väisälä Foundation for financial support. The authors acknowledge the reviewers for their constructive comments and suggestions.

References

[1] Janhunen, P., "Electric Sail for Spacecraft Propulsion," *Journal of Propulsion and Power*, Vol. 20, No. 4, 2004, pp. 763–764.

[2] Janhunen, P., and Sandroos, A., "Simulation Study of Solar Wind Push on a Charged Wire: Basis of Solar Wind Electric Sail Propulsion," *Annales Geophysicae*, Vol. 25, No. 3, 2007, pp. 755–767.

[3] Hoyt, R. P., and Forward, R. L., "Alternate Interconnection Hoytether Failure Resistant Multiline Tether," U.S. Patent 6286788, Issued 11 Sept. 2001.

[4] Forward, R. L., and Hoyt, R. P., "Failsafe Multiline Hoytether Lifetimes," 31th AIAA/ASME/SAE/ASEE Joint Propulsion Conference and Exhibit, San Diego, CA, AIAA Paper 1995-2890, 10–12 July 1995.

[5] Forward, R. L., and Nordley, G. D., "Mars-Earth Rapid Interplanetary Tether Transport (MERITT) System, 1: Initial Feasibility Analysis," 35th AIAA/ASME/SAE/ASEE Joint Propulsion Conference and Exhibit, Los Angeles, AIAA Paper 1999-2151, 20–24 June 1999.

[6] Hoyt, R. P., "Commercial Development of a Tether Transport System," 36th AIAA/ASME/SAE/ASEE Joint Propulsion Conference and Exhibit, Huntsville, AL, AIAA Paper 2000-3842, 16–19 July 2000.

[7] Hoyt, R. P., "Design and Simulation of a Tether Boost Facility for LEO to GTO Transport," 36th AIAA/ASME/SAE/ASEE Joint Propulsion Conference and Exhibit, Huntsville, AL, AIAA Paper 2000-3866, 16–19 July 2000.

[8] Whang, Y. C., "A Solar-Wind Model Including Proton Thermal

Anisotropy," *The Astrophysical Journal*, Vol. 178, Nov. 1972, pp. 221–240.
doi:10.1086/151782

[9] Sittler, E. C., and Scudder, J. D., "An Empirical Polytrope Law for Solar Wind Thermal Electrons Between 0.45 and 4.76 AU: Voyager 2 and Mariner 10," *Journal of Geophysical Research*, Vol. 85, Oct. 1980, pp. 5131–5137.

[10] Slavin, J. A., and Holzer, R. E., "Solar Wind Flow about the Terrestrial Planets, 1. Modeling Bow Shock Position and Shape," *Journal of Geophysical Research*, Vol. 86, No. 11, Dec. 1981, pp. 11401–11418.

[11] Koppel, C. R., and Estublier, D., "The SMART-1 Electric Propulsion Subsystem," 39th AIAA/ASME/SAE/ASEE Joint Propulsion Conference & Exhibit, Huntsville, AL, AIAA Paper 2003-4545, 20–23 July 2003.

[12] Milligan, D., Camino, O., and Gestal, D., "SMART-1 Electric Propulsion: An Operational Perspective," 9th International Conference on Space Operations, Rome, AIAA Paper 2006-5767, 19–23 June 2006.

[13] Dachwald, B., "Solar Sail Performance Requirements for Missions to the Outer Solar System and Beyond," *55th International Astronautical Congress, Vancouver, Canada*, International Astronautical Congress Paper 04-S.P.11, 04–08 Oct. 2004.

[14] Mengali, G., and Quarta, A. A., "Solar-Sail-Based Stopover Cyclers for Cargo Transportation Missions," *Journal of Spacecraft and Rockets*, Vol. 44, No. 4, July–Aug. 2007, pp. 822–830.
doi:10.2514/1.24423

[15] Bryson, A. E., and Ho, Y. C., *Applied Optimal Control*, Hemisphere, New York, NY, 1975, pp. 71–89, Chap. 2.

[16] Lawden, D. F., *Optimal Trajectories for Space Navigation*, Butterworths, London, 1963, pp. 54–68.

[17] Russell, R. P., "Primer Vector Theory Applied to Global Low-Thrust Trade Studies," *Journal of Guidance, Control, and Dynamics*, Vol. 30, No. 2, Mar.–Apr. 2007, pp. 460–472.
doi:10.2514/1.22984

[18] Wright, J. L., *Space Sailing*, Gordon and Breach Science Publisher, Berlin, 1992, pp. 227–233.

[19] Mengali, G., and Quarta, A. A., "Optimal Three-Dimensional Interplanetary Rendezvous Using Nonideal Solar Sail," *Journal of Guidance, Control, and Dynamics*, Vol. 28, No. 1, Jan.–Feb. 2005, pp. 173–177.

[20] Dachwald, B., Mengali, G., Quarta, A. A., and Macdonald, M., "Parametric Model and Optimal Control of Solar Sails with Optical Degradation," *Journal of Guidance, Control, and Dynamics*, Vol. 29, No. 5, Sept.–Oct. 2006, pp. 1170–1178.

B. Marchand
Associate Editor